Energy loss of hydrogen atoms colliding with glycine at low impact energies: Electronic, nuclear, and rovibrational contributions

C. Martínez-Flores[a], F. J. Domínguez-Gutiérrez[b], R. Cabrera-Trujillo[c,*]

[a]*Departamento de Química, División de Ciencias Básicas e Ingeniería, Universidad Autónoma Metropolitana-Iztapalapa, San Rafael Atlixco 186, Col. Vicentina, Iztapalapa C. P. 09340, Ciudad de México, México*

[b]*Max-Planck-Institute for Plasma Physics, Boltzmannstrasse 2, 85748 Garching, Germany*

[c]*Instituto de Ciencias Físicas, Universidad Nacional Autónoma de México, Ap. Postal 43-8, Cuernavaca, Morelos, 62251, México*

Abstract

The study of the energy deposition of neutral hydrogen on biomolecules is of great importance in the determination of cell damage by irradiation with heavy ions. In this work, we report the energy loss of hydrogen atoms when colliding on glycine molecule in gas phase. Our study has as a central role the comparison of the Density-Functional Tigth-Binding (DFTB) which is a quantum-classical molecular dynamics (QCMD) approach, valid in the low collision energy region, to the Electron-Nuclear Dynamics (END) theory which accounts for electron and nuclear couplings in the dynamics and is an ab initio quantum chemistry approach. These two approaches have an overlap collision energy region from 10 to 100 eV. Our results show that both approaches complement each other very well. We find that the electronic stopping cross-section shows a linear velocity dependence with a threshold at 0.01414 a.u. corresponding to around 5 eV for END, while the same threshold is shown by the DFTB results but around 1 eV. At that collision energy, the ro-vibrational, nuclear, and molecular fragmentation (collision induced damage) energy loss becomes very important. Finally, we compare with available theoretical and experimental data showing the good agreements of our results.

Keywords: Glycine molecule, Molecular dynamics, SCC-DFTB, Energy loss, Stopping cross section, Electron-Nuclear Dynamics

1. Introduction

The energy loss of ions in matter has been a topic of interest since the pioneering work of Bohr and Bethe for the high energy collisions with promises in applications on the industry, medicine, and materials science [1]. However, in recent years the study of biological material damage by energy deposition of fast ions has shown an increase due to direct applications on medical treatments, e.g. radiation therapy [2]. Here, the biological damage is accounted for slow and fast ions where the major energy deposition (projectile energy loss) is desirable. At a molecular level, the projectile ions collide with DNA strand, organic compounds, e.g. amines, amino acids or nucleobases, among others [3, 4]. In this work, we are interested in the study of the energy deposition of hydrogen atoms on the glycine amino acid at low collision energies.

The glycine molecule (NH_2CH_2COOH) is the simplest amino acid naturally found in proteins and widely used in the pharmaceutical industry as the active ingredient [5]. In combination with carbon nanotubes, there is a promise in applications as biochemical sensors, drug delivery, and therapeutic applications [6]. The glycine molecule has been studied with methods based on the density functional theory (DFT), Hartree-Fock methods, Self-Consistent Charge Density Functional Tight-Binding (SCC-DFTB), among others [7, 8, 9, 10, 11, 12, 13, 14]. For example, Kaschner et al. [8] implement the DTF theory with a plane-wave pseudopotential scheme to calculate the relative energies and geometries for the glycine molecule finding good agreement with experimental results and post-Hartree-Fock calculations. Lin et al. [9] studied the neutral glycine molecule in gas phase with the DFT theory reporting accurate geometries and relative energies in good agreement with previous theoretical and experimental results. Elstner et al. [11] studied the relative energies and geometries of the glycine and alanine based polypeptides with several theoretical methods as the Hartree-Fock (HF), MP2, SCC-DFTB, and DFT approaches. Furthermore, Elstner et al. [11] find results reliably when comparing DFTB to those obtained with DFT. Oliveira et al. [12] show results for dipolar ion of glycine molecule in aqueous solution using a dispersion-corrected SCC-DFTB Hamiltonian. Zhao et al. [13] show results for the glycine dipolar ion interacting with a silica surface with molecular dynamic simulations based on density functional tight-binding method finding favorable adsorption conformation of the glycine amino acid. Zhai et al. [14] implement the SCC-DFTB approach to study a dipolar ion to study the impact of water environment on the molecular structure finding a stabilization processes by the medium water.

With respect to energy deposition, there has been a limited number of studies for hydrogen atoms colliding with glycine at high collision energies. Abril et al. [3] has used Lindhard's dielectric theory [15] to study the stopping cross section of protons and helium ions collisions on DNA for energies above the

*Corresponding author

Email address: trujillo@icf.unam.mx (R. Cabrera-Trujillo)

maximum of the curve. Similarly, Tan et al. [4] has used a Mermin description of the dielectric function to study the energy deposition of protons colliding with some biological molecules. However, there is no experimental work on this amino acid for the stopping cross section nor a theoretical study of energy deposition at low collision energy, to the authors' knowledge.

In this work, we are interested in studying the total, electronic, nuclear, and roto-vibrational stopping cross section (energy deposition) of hydrogen atoms on glycine molecule in gas phase implementing the SCC-DFTB quantum classical molecular dynamics and the END ab initio quantum chemistry approach. To our knowledge, there is no literature reporting the stopping cross section of hydrogen atoms on glycine molecule at low collision energies.

Our work is presented with the following structure: In section 2, we briefly describe the Self-Consistent Charge Density-Functional Tight-Binding (SCC-DFTB) method and the END approach. Also, we discuss the preparation of the glycine target to perform Quantum-Classical Molecular Dynamics (QCMD) simulations to emulate hydrogen irradiation on this molecule. In Section 3, we present the results of the energy loss distribution and stopping power cross-section at different impact energies, which are calculated by both theories. Finally, in section 4, we give our concluding remarks.

2. Theory

The Self-Consistent Charge Density Functional Tight-Binding (SCC-DFTB) method is an approximation to the conventional density functional theory (DFT), where only valence electron interactions are explicitly considered [16]. The Kohn-Sham (KS) equations are solved for the total valence electronic densities and energies using a predetermined Hamiltonian, which is constructed on the basis of a two-center approximation with optimized pseudo-atomic orbitals as basis functions. Tabulated Hamiltonian matrix elements, overlap integrals, and repulsive splines fitted to DFT dissociation curves of reference molecular systems are contained in the Slater-Koster parameter files (SKF) [16, 17] and are read into computer memory only once during the QCMD simulation runs. In this study, we utilize the SKF pair potentials set for biological science simulations (OB2-1-1) [18] that includes long range corrections. The electronic energies are calculated as a sum over the occupied KS single-particle energies and the sum over diatomic repulsive energy contributions. Self-Consistent Charge (SCC) corrections, as implemented in the DFTB+ code [19], are included in the total energy via an iteration procedure that converges to a new electron density at every time step during a QCMD simulation, where the convergence is improved by using an electronic temperature of 1000 K. The SCC-DFTB approach as implemented in the publicly available DFTB+ code [19] version 1.2 and is used in this work for the geometry optimizations and QCMD simulations.

The other method we use in this work is the Electron-Nuclear Dynamics (END) [20] which solves the time-dependent Schrödinger equation with the nuclei and electrons coupled. END uses a parametrization of the wave function in a coherent-state manifold, which leads to a system of Hamilton's equations of motion [21]. The variational wave function is a molecular generalized coherent state represented by coupled electronic and nuclear wave functions. The simplest implementation of the END approach employs a single spin-unrestricted electronic determinant written in terms of non-orthogonal spin orbitals whose ξ coefficients describe the electron dynamics. These electronic molecular orbitals are in turn expressed in terms of a basis of augmented Gaussian atomic-type orbitals of rank K with complex coefficients. The Gaussian-type orbitals are centered on the average positions $\mathbf{R}$ of the participating atomic nuclei which are moving with momentum $\mathbf{P}$. This representation takes into account the momentum of the electrons explicitly by means of electron translation factors [22]. The nuclear part of the wave function is represented by localized Gaussian functions, which in the narrow wave-packet limit become classical trajectories. The dynamical equations that describe the time-evolution of the wave-function, include the non-adiabatic coupling terms between the electrons and nuclei. Solving the set of equations for $\{\xi, \mathbf{R}, \mathbf{P}\}$ as a function of the time generates the evolving molecular state that describes the processes that take place during the collision. This scheme has been implemented in the ENDyne program package [21]. One advantage of the END approach is that it treats excited states, however, this method is computationally costly at low collision energies.

From the calculations, we obtain the following row data as a function of the impact parameter, b: the scattering angle, θ_s of the projectile; number of projectile electrons, N_e; the projectile energy loss, ΔE_n; and initial and final velocity relation, v_f/vi (inelasticity of the collision). The projectile energy loss is defined as $\Delta E = E_f - E_i$, where E_i and E_f are the initial and final kinetic energies of the projectile center of mass, respectively.

The differential cross section for the projectile scattering is defined as

$$\frac{d\sigma}{d\Omega} = \frac{b}{\sin\theta}\left|\frac{db}{d\theta}\right| = \frac{b}{\sin\theta}\frac{1}{\left|\frac{d\theta}{db}\right|}\,. \tag{1}$$

Consequently, the electronic stopping cross section, as a function of the impact collision energy, is given as

$$S_e = \int \Delta E \frac{d\sigma}{d\Omega} d\Omega = 2\pi \int b\Delta E_n db\,. \tag{2}$$

As the glycine molecule is a multi-center system, we can determine the energy loss of the projectile onto the glycine. Furthermore, due to energy conservation, the projectile energy loss is absorbed as: electronic excitations, nuclear target recoil (nuclear energy loss), and rotational and vibrational target excitations. As the details of these energy loss contributions have been already reported by one of the authors [23], here we only report the final results.

2.1. Hydrogen irradiation on a glycine molecule

The glycine molecule is optimized previous computer simulations and calculations within both approaches. As the main goal is to compare DFTB+ and END, we have chosen to perform the dynamics at the zero-point geometry configuration,

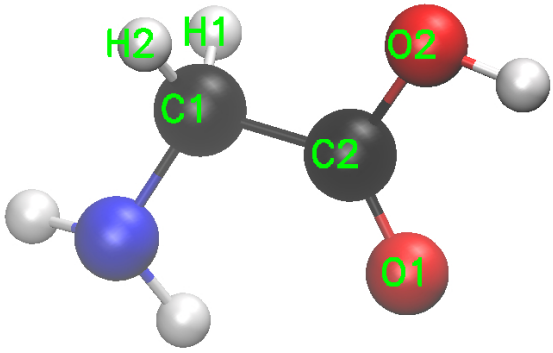

Figure 1: (Color on-line). The optimized structure of the glycine molecule used in this work. The atoms are represented by colored spheres as: C in black, N in blue, O in red, and H in white.

Table 1: Bond lengths of the glycine molecule obtained after an optimization process by the SCC-DFTB and END method (See Fig. 1). The values within parenthesis correspond to the END geometry optimization at the HF-SCF level.

Bond	Length (Å)	Bond	Length (Å)
C(1)–C(2)	1.52	C(1)–H(2)	1.09
	(1.55)		(1.09)
C(1)–N	1.51	C(1)–H(2)	1.10
	(1.48)		(1.11)
C(2)=O(1)	1.23	N–H	1.01
	(1.22)		(1.03)
C(2)–O(2)	1.39	N–H	1.01
	(1.37)		(1.02)
O(2)–H	0.97		
	(0.97)		

that is, no thermalization is used prior to irradiation by hydrogen atoms. In Fig. 1, we show the optimized structure of the glycine molecule. In Table 1, the bond lengths are given in units of Å, as obtained by both approaches. For the END method, a STO-3G basis set from Pople et al. [24] has been used and the geometry optimization has been achieved by a SCF approach.

The glycine molecule is bombarded with 923 hydrogen atoms that are distributed on the six faces of a cube with the glycine molecule center of mass at the center of the cube in order to account for the random orientation of the target molecule. The projectile's impact parameter, b, is distributed along the four axes on each face of the cube reference system, as shown in Fig. 2. The impact parameter runs from $b = 0.0$ to 20 a.u. (≈ 11 Å and the projectile is placed at an initial distance of 15 Å measured from the glycine's center of mass. In Fig. 2, we show the hydrogen atoms and glycine molecule initial collision positions.

For the dynamics of the collision, we consider the following impact energies: 1, 2.5, 5, 10, 20, 30, 50, and 100 eV with the DFTB+ approach and 10, 20, 30, 50, 100, 250, 500, and 1000 eV with the Electron-Nuclear Dynamics approach. For the collision dynamic with DFTB+, we use the velocity Verlet algorithm with a time step of 0.05 fs.

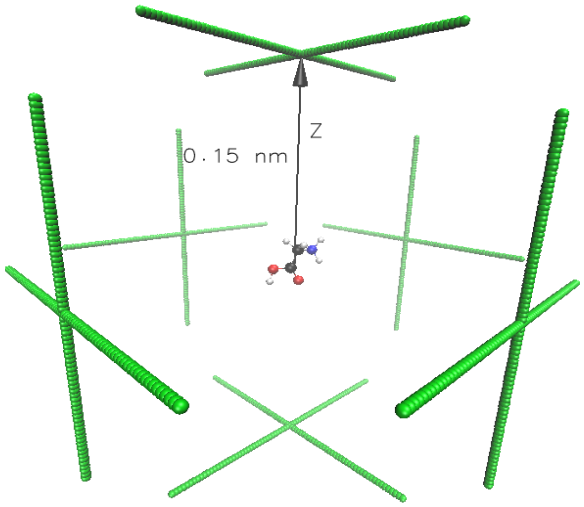

Figure 2: (Color on-line). Perspective view of the initial position of the H projectiles when colliding with a glycine molecule. The center of mass of the target is at the origin of the coordinate system. Color code: H impact are illustrated as green spheres, meanwhile glycine molecule follows the color code used in Fig. 1

3. Results

3.1. Projectile energy loss

In Fig. 3, we show the energy loss, weighted by the impact parameter for neutral hydrogen atoms when colliding with a glycine molecule as a function of the impact parameter. In Fig. 3a), we show the results as obtained by the DFTB+ approach for the hydrogen collision energies of 5, 10, 20, 30, 50, and 100 eV. The ($\circ$) symbols represent all the impacts for all the target orientations. The red solid line is the averaged — over the same impact parameter — energy loss and allows to determine the averaged stopping cross section. Note that as the collision energy increases, the energy loss increases for the same impact parameter. The highest impact parameter contribution occurs around $b \sim 3$ to 4 a.u. . In Fig. 3b), we show the results obtained by the END approach for the collision energies of 10, 50, 100, 250, 500, and 1000 eV. The results show that in average, both approaches produce similar results for the collision energies between 10 to 50 eV. As the collision energy increases, larger projectile energy loss occurs for impact parameters around 3 to 4 a.u. similarly to the DFTB results.

In Fig. 4, we show the energy-loss distribution of the hydrogen atoms scattered by the glycine molecule as a function of the projectile energy loss, ΔE, averaged over all the target orientations for the collision energies of 10, 20, 30, 50, and 100 eV. The red solid line is a spline fit to guide the eye. In Fig. 4a), we show the results obtained by the DFTB+ approach. At 10 eV, we find a gaussian envelope for the distribution that peaks around 0.1 a.u. in energy loss and a width of 0.2 a.u. that is around 5.4 eV corresponding to the averaged energy deposited into the Glycine molecule. A similar result, although with a broader width is obtained with the END approach, as seen in Fig. 4b). Similar results are obtained at 20 and 30 eV for both approaches with a wider distribution, which corresponds to a

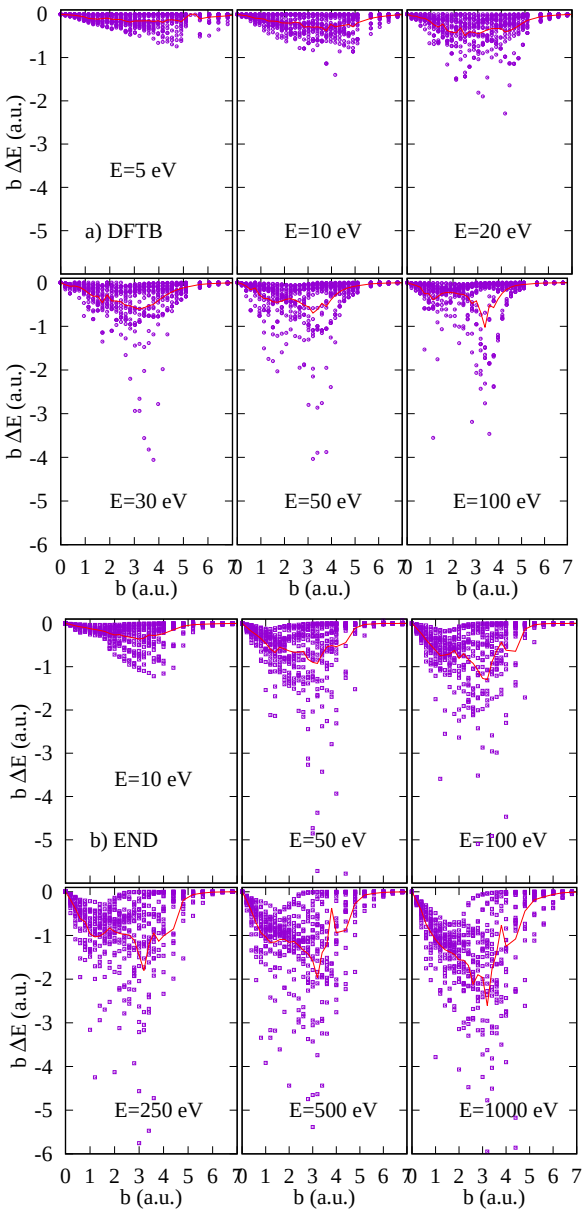

Figure 3: (Color on-line). Energy loss, weighted by the impact parameter for H atoms colliding with a glycine molecule, as a function of projectile impact parameter for all the target orientations. In a) we show the results as obtained with the DFTB+ approach and in b) we show the results obtained by END. The solid red line is the average over all the target orientations. See text for details.

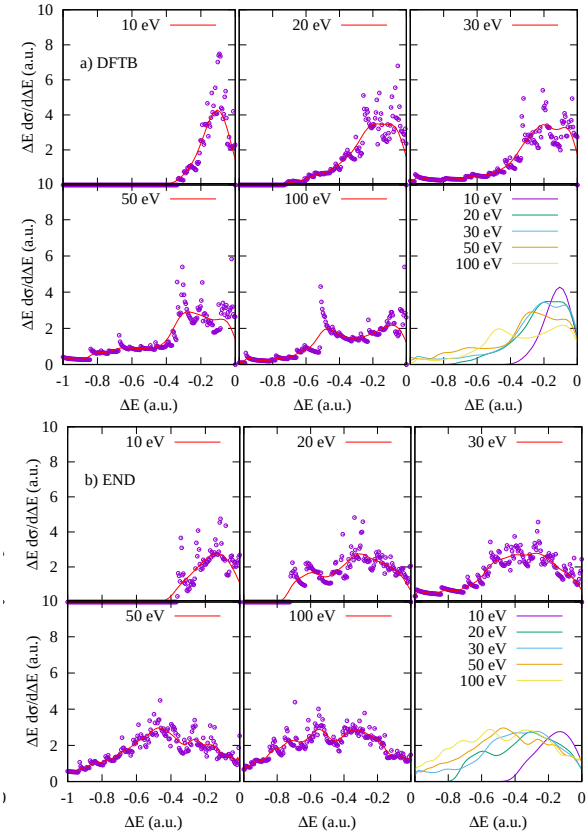

Figure 4: (Color on-line). Energy loss distribution (intensity of scattered particles), weighted by the projectile energy loss, for H atoms colliding with glycine as a function of projectile energy loss and averaged over all the target orientations. In a), we show the results obtained by the DFTB approach and in b) as obtained by the END method. The solid line that goes through the points is an adjusted curve to guide the eye. In the last frame we show these lines for comparison. See text for details.

larger energy deposited to the target as the projectile collision energy increases. However, for collision energies larger than 50 eV, END produces a wider and large energy loss distribution, as observed in the last frame.

In Fig. 5, we show the total, electronic, nuclear, and rovibrational stopping cross-section for hydrogen atoms colliding with a glycine molecule as a function of the projectile velocity, as obtained with both approaches. In Fig. 5a), we show the results obtained by the DFTB+ approach. The purple solid line is the total stopping cross section. The symbols represent the actual calculated velocities. Interestingly, it shows a maximum at around 0.04 a.u., which corresponds to a projectile collision energy of 50 eV. For higher collision energies, the stopping cross section diminishes. In the same figure, we show the nuclear energy loss (blue short-dashed line with symbols), that is, the kinetic energy gained by the glycine target center of mass. The dotted long-dash line with (□) symbols shows the rovibrational stopping cross section, which accounts for the energy gained by the target and distributed in the glycine molecule as rotations and vibrations. Finally, in the same figure, we show the electronic contribution, that is, the energy deposited in the glycine molecule consequence of the target electronic density effects. Strictly speaking, the electronic contribution, it is not due to excitations, since DFTB does not account for them, but it is due to electronic density deformations or polarization of the electronic cloud, as the SCC-DFTB accounts for. Interestingly, it shows a threshold around 0.007 a.u. in the projectile velocity, or around 1.2 eV. For $0.007 < v < 0.03$ a.u. which corresponds to $1 < E < 20$ eV of collision energy, the stopping cross section shows a linear behaviour, in agreement to theoretical predictions [25, 26]. For higher collision energies, it starts to diminish. In Fig. 5b), we show the stopping cross section of the hydrogen atom when is colliding on Glycine molecule as obtained with the END approach as a function of the pro-

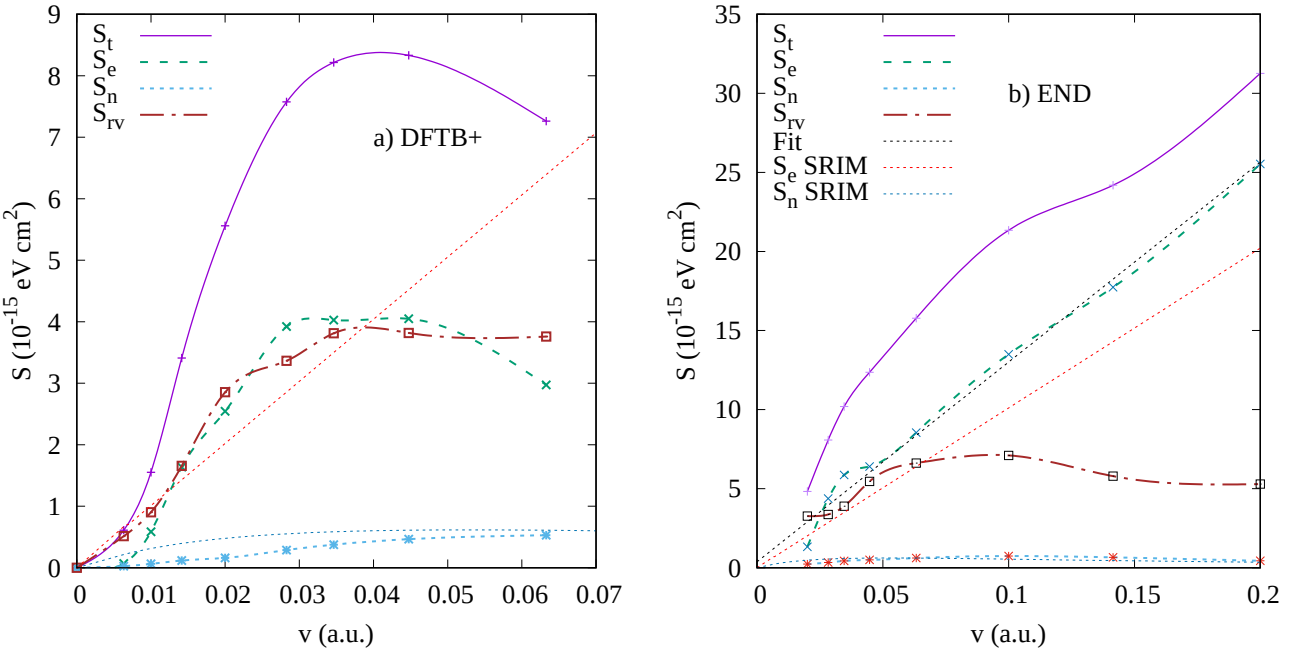

Figure 5: (Color on-line). Total, electronic, nuclear, and ro-vibrational stopping cross section for H atoms colliding with a glycine molecule, as a function of projectile initial velocity. In a), we show the DFTB+ results and in b) the END method. The dotted red lines is the electronic stopping cross section as obtained with SRIM [25] and the dotted blue line is the corresponding nuclear contribution from SRIM. See text for details.

jectile initial velocity. In the same figure, we show the energy gained by the glycine target molecule as ro-vibrational, nuclear displacement, and electronic excitations. However, in this case, the total stopping cross section keeps increasing as a function of the projectile velocity. For collision velocities from 0.05 to 0.2 a.u., the electronic stopping cross section show a linear behavior, although it shows a bump around 0.03 a.u. or 23 eV and a threshold around 0.015 a.u. which corresponds to a collision energy of 5.6 eV. . These last effects seem in agreement to the target electronic cloud polarization shown by the DFTB results. In the same figure, we show the results from SRIM [25] (red dotted line) for comparison purposes. We observe that SRIM underestimates the electronic stopping cross section at low collision energies. In the same figure, we show an adjusted line to our electronic stopping cross section (black dotted line). We find that $S_e = 126.332v + 0.375635$ eV cm^2 and valid for $v > 0.05$ a.u. when SRIM predicts that $S_e = 101.05v$ eV cm^2. For the case of the nuclear stopping cross, we find that the END results and those of SRIM agree completely.

Finally, in Fig. 6, we show the comparison of all the stopping cross sections obtained by the DFTB and END approaches in the overlap energy region. We observe that for collision velocities below 0.03 a.u., the END and DFTB results compare fairly well, particularly for the ro-vibrational contribution. Even more, the nuclear stopping cross section compares very well for up to collision velocities of 0.06 a.u. or 100 eV. However, the electronic contribution is different, mostly due to the lack of low excitation states in the DFTB approach. In general, we conclude that both approaches complement very well. The DFTB approach can be used for collision velocities below 0.03 a.u. or 30 eV. For higher collision energies, then higher excited states start to play a role and END or any theory that accounts for excitations should be used.

4. Conclusions

In this paper, we performed QCMD simulations by the SCC-DFTB method as well as Electron-Nuclear Dynamics to study

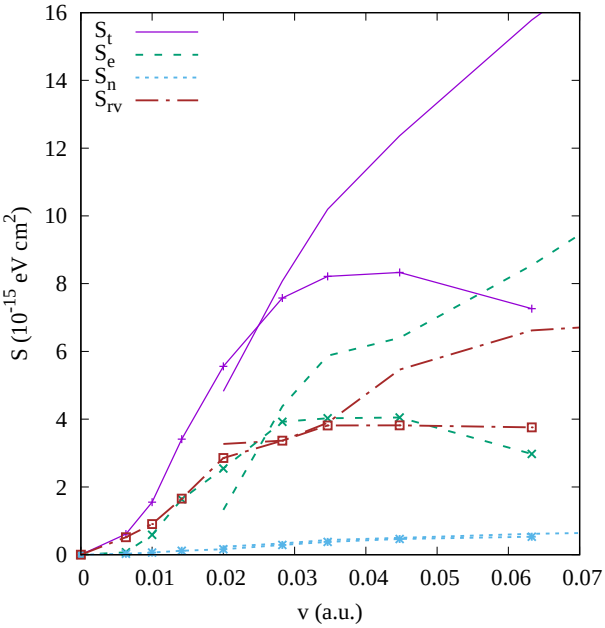

Figure 6: (Color on-line). Comparison of END and DFTB+ stopping cross section for H colliding on Glycine as a function of the projectile velocity. The lines with symbols correspond to the DFTB+ results. The lines with the same color and no symbols correspond to the END results. See text for details.

the energy loss of H atoms colliding with a glycine molecule in the impact energy range 1-100 eV for DFTB and 10-1000 eV for the END approach. We find that both approaches complement each other with the DFTB doing a good job at collision energies lower than 30 eV and END performing well for all the collision energies. The DFTB is a fast approach while the END is computationally costly but privides the full quantum wave-function for the system. We find that both approaches agree when reporting the nuclear stopping cross section. The DFTB does not accounts for excitations, however it does a good description of polarization effects induced onto the electronic ground state wave-function. Furthermore, both approaches agree in finding a threshold effect in the electronic stopping cross section. For DFTB approach, the threshold occurs at 2 eV while for the END it predicts a threshold around 5 eV (0.01 and 0.01415 a.u. for the velocity, respectively). When comparing to the SRIM code, we find that it underestimates by 10% the electronic stopping cross section and it completely neglects the ro-vibrational stopping cross section. Consequently, a larger energy loss and stopping cross section is found at low collision energies with our approaches than with SRIM.

Acknowledgments

We acknowledge support from DGAPA-UNAM PAPIIT-IN-106-617 and LANCAD-UNAM-DGTIC-228 to RCT. CMF thanks CONACyT for the postdoctoral fellowship through the project FC-2016/2412. FJDG acknowledges the A. von Humboldt Foundation for a research fellowship. Partial results in this paper were obtained using the Seawolf institutional cluster at the Institute for Advanced Computational Science at Stony Brook University and ICF-UNAM research group cluster.

References

[1] A. V. Solov'yov (Ed.), Nanoscale Insights into Ion-Beam Cancer Therapy, Springer, Cham, Springer International Publishing Switzerland, 2017. doi:10.1007/978-3-319-43030-0.
URL https://doi.org/10.1007/978-3-319-43030-0

[2] J. R. Sabin, E. Brändas, Advances in Quantum Chemistry, Vol. 52, Academis Press, USA, 2007.
URL https://www.sciencedirect.com/bookseries/advances-in-quantum-chemistry/vol/52/suppl/C

[3] I. Abril, R. García-Molina, C. C. Denton, I. Kyriakou, D. Emfietzoglou, Energy loss of hydrogen and helium-ion beams in dna: Calculation based on a realistic energy-loss function of the target, Rad. Res. 175 (2) (2011) 247. doi:10.1667/RR2142.1.
URL https://doi.org/10.1667/RR2142.1

[4] Z. Tan, Y. Xia, M. Zhao, X. Liu, Electronic stopping power for proton in amino acids and protein in 0.0510 mev range, Nucl. Instr. Meth. Phys. Res. B 266 (9) (2008) 1938 – 1942. doi:10.1016/j.nimb.2008.03.043.
URL https://doi.org/10.1016/j.nimb.2008.03.043

[5] Y. Yani, P. S. Chow, R. B. H. Tan, Glycine open dimers in solution: New insights into -glycine nucleation and growth, Crystal Growth & Design 12 (10) (2012) 4771–4778. arXiv:https://doi.org/10.1021/cg300452n, doi:10.1021/cg300452n.
URL https://doi.org/10.1021/cg300452n

[6] A. Mavrandonakis, S. C. Farantos, G. E. Froudakis, Glycine interaction with carbon nanotubes: an ab initio study, The Journal of Physical Chemistry B 110 (12) (2006) 6048–6050, pMID: 16553415. arXiv:https://doi.org/10.1021/jp057296l, doi:10.1021/jp057296l.
URL https://doi.org/10.1021/jp057296l

[7] A. G. Csaszar, Conformers of gaseous glycine, Journal of the American Chemical Society 114 (24) (1992) 9568–9575. arXiv:https://doi.org/10.1021/ja00050a041, doi:10.1021/ja00050a041.
URL https://doi.org/10.1021/ja00050a041

[8] R. Kaschner, D. Hohl, Density functional theory and biomolecules: a study of glycine, alanine, and their oligopeptides, The Journal of Physical Chemistry A 102 (26) (1998) 5111–5116. arXiv:https://doi.org/10.1021/jp980975u, doi:10.1021/jp980975u.
URL https://doi.org/10.1021/jp980975u

[9] P. Li, Y. Bu, H. Ai, Conformational study of glycine amide using density functional theory, The Journal of Physical Chemistry A 107 (33) (2003) 6419–6428. arXiv:https://doi.org/10.1021/jp034886f, doi:10.1021/jp034886f.
URL https://doi.org/10.1021/jp034886f

[10] R. Maul, F. Ortmann, M. Preuss, K. Hannewald, F. Bechstedt, Dft studies using supercells and projector-augmented waves for structure, energetics, and dynamics of glycine, alanine, and cysteine, Journal of Computational Chemistry 28 (11) (2007) 1817–1833. arXiv:https://onlinelibrary.wiley.com/doi/pdf/10.1002/jcc.20683, doi:10.1002/jcc.20683.
URL https://onlinelibrary.wiley.com/doi/abs/10.1002/jcc.20683

[11] M. Elstner, K. J. Jalkanen, M. Knapp-Mohammady, T. Frauenheim, S. Suhai, Energetics and structure of glycine and alanine based model peptides: Approximate scc-dftb, am1 and pm3 methods in comparison with dft, hf and mp2 calculations, Chemical Physics 263 (2) (2001) 203 – 219. doi:https://doi.org/10.1016/S0301-0104(00)00375-X.
URL http://www.sciencedirect.com/science/article/pii/S030101040000375X

[12] A. F. Oliveira, G. Seifert, T. Heine, H. A. A. Duarte, Density-functional based tight-binding: an approximate dft method, Journal of the Brazilian Chemical Society 20 (2009) 1193 – 1205.
URL http://www.scielo.br/scielo.php?script=sci_arttext&pid=S0103-50532009000700002&nrm=iso

[13] Y. L. Zhao, S. Kppen, T. Frauenheim, An scc-dftb/md study of the adsorption of zwitterionic glycine on a geminal hydroxylated silica surface in an explicit water environment, The Journal of Physical Chemistry C 115 (19) (2011) 9615–9621. arXiv:https://doi.org/10.1021/jp200610p, doi:10.1021/jp200610p.
URL https://doi.org/10.1021/jp200610p

[14] Y. Zhai, Y. L. Zhao, A self-consistent-charge density-functional tight-binding theory based molecular dynamics simulation of a zwitterionic glycine in an explicit water environment, Journal of Theoretical and Computational Chemistry 12 (04) (2013) 1350019. arXiv:https://doi.org/10.1142/S0219633613500193, doi:10.1142/S0219633613500193.
URL https://doi.org/10.1142/S0219633613500193

[15] J. Lindhard, M. Scharff, Energy loss in matter by fast particles of low charge, Kgl. Dan. Vidensk. Selsk. Mat. Fys. Medd. 27 (1953) 1–32.

[16] M. Elstner, D. Porezag, G. Jungnickel, J. Elsner, M. Haugk, T. Frauenheim, S. Suhai, G. Seifert, Self-consistent-charge density-functional tight-binding method for simulations of complex materials properties, Phys. Rev. B 58 (1998) 7260–7268. doi:10.1103/PhysRevB.58.7260.
URL https://link.aps.org/doi/10.1103/PhysRevB.58.7260

[17] B. Lukose, A. Kuc, J. Frenzel, T. Heine, On the reticular construction concept of covalent organic frameworks, Beilstein J. Nanotechnol. 1 (2010) 6070. doi:10.3762/bjnano.1.8.

[18] V. Q. Vuong, J. Akkarapattiakal Kuriappan, M. Kubillus, J. J. Kranz, T. Mast, T. A. Niehaus, S. Irle, M. Elstner, Parametrization and benchmark of long-range corrected dftb2 for organic molecules, Journal of Chemical Theory and Computation 14 (1) (2018) 115–125, pMID: 29232515. arXiv:https://doi.org/10.1021/acs.jctc.7b00947, doi:10.1021/acs.jctc.7b00947.
URL https://doi.org/10.1021/acs.jctc.7b00947

[19] http://www.dftb-plus.info/ (2017).

[20] E. Deumens, Y. hrn, Complete electron nuclear dynamics, The Journal of Physical Chemistry A 105 (12) (2001) 2660–2667. doi:10.1021/jp003824b.

[21] E. Deumens, T. Helgaker, A. Diz, H. Taylor, J. Oreiro, B. Mogensen, J. A. Morales, M. C. Neto, R. Cabrera-Trujillo, D. Jacquemin, ENDyne version 2.8 Software for Electron Nuclear Dynamics, Quan-

tum Theory Project, University of Florida, Gainesville FL 32611-8435, http://www.qtp.ufl.edu/ deumens/endyne.html (2000).

[22] E. Deumens, A. Diz, R. Longo, Y. Öhrn, Time-dependent theoretical treatments of the dynamics of electrons and nuclei in molecular systems, Rev. Mod. Phys. 66 (1994) 917–983. doi:10.1103/RevModPhys.66.917.
URL https://link.aps.org/doi/10.1103/RevModPhys.66.917

[23] R. Cabrera-Trujillo, Y. Öhrn, E. Deumens, J. R. Sabin, Trajectory and molecular binding effects in stopping cross section for hydrogen beams on h_2, J. Chem. Phys. 116 (2002) 2783. doi:10.1063/1.1436107.
URL https://doi.org/10.1063/1.1436107

[24] W. J. Hehre, R. F. Stewart, J. A. Pople, Selfconsistent molecularorbital methods. i. use of gaussian expansions of slatertype atomic orbitals, The Journal of Chemical Physics 51 (6) (1969) 2657–2664. arXiv:https://doi.org/10.1063/1.1672392, doi:10.1063/1.1672392.
URL https://doi.org/10.1063/1.1672392

[25] J. F. Ziegler, J. P. Biersack, U. Littmark, The Stopping and Range of Ions in Solids, Pergamon Press, New York, 1985.
URL http://www.srim.org

[26] E. Fermi, E. Teller, The capture of negative mesotrons in matter, Phys. Rev. 72 (1947) 399–408. doi:10.1103/PhysRev.72.399.
URL https://link.aps.org/doi/10.1103/PhysRev.72.399